



INTER-INFLUENCE OF DEFECTS IN WELDED JOINT ZONE AT DIFFERENT FORCE LOADING

V.I. MAKHNENKO, E.A. VELIKOIVANENKO, A.S. MILENIN, G.F. ROZYNKA and N.I. PIVTORAK
E.O. Paton Electric Welding Institute, NASU, Kiev, Ukraine

It is noted that force interaction of group discontinuity defects of material in welded structures is not necessarily reduced to the concept, according to which the adjacent defect impairs the service load resistance or does not affect it at a sufficiently large distance between them. A variant is considered, when interaction of group defects of the type of cracks or wall thinning defects, improves the resistance to service loading.

Keywords: welded joints, group defect interaction, parallel defects, collinear defects, fracture probability

Extent of damage of a particular structure under specific service conditions is usually determined by the number of found inadmissible defects. It is natural that the greater the number of such defects, the more damaged the examined structure is believed to be. The existing rules of allowing for inter-influence of defects [1–3, etc.] are usually reduced to combining by the respective rules two or more admissible defects located closest to each other into one independent admissible (inadmissible) defect based on a concept, according to which the neighbouring defect impairs or does not influence the service load resistance of this defect.

Such a concept is quite simple, but on the whole it is too conservative in a number of cases, as it does not allow for the possibility of a third alternative, namely that the neighbouring defect can unload this defect, and thus, improve its performance under specific service conditions.

Allowing for the third alternative at engineering diagnostics of structures requires application of the appropriate calculation procedures, normative documents, etc. but, nonetheless, considering the modern tendencies in development of computer engineering,

methods of mathematical modeling, information systems, as well as growing requirements to optimization of the developed critical structures, the good prospects for application of these developments are undoubtful, particularly for prediction of safe operation of welded structures with long service life by the results of the respective engineering diagnostics of their state.

This paper deals with such a possibility for sufficiently characteristic in-service defects of welded structures in the form of cracks and thinning.

Let us start with the simplest examples of interaction of two and three through-thickness parallel cracks of the same dimensions in an unlimited plate, uniformly tensioned along a normal to crack plane (Figures 1 and 2) by stress σ . The characteristic of such defect loading is the stress intensity factor in crack tip K_I . Respective data from [4] for the case of two cracks are given in Figure 1 and in Table 1, and those for three cracks – in Figure 2, depending on distance between cracks d . These data show that d decrease noticeably lowers K_I values, both for two and for three cracks.

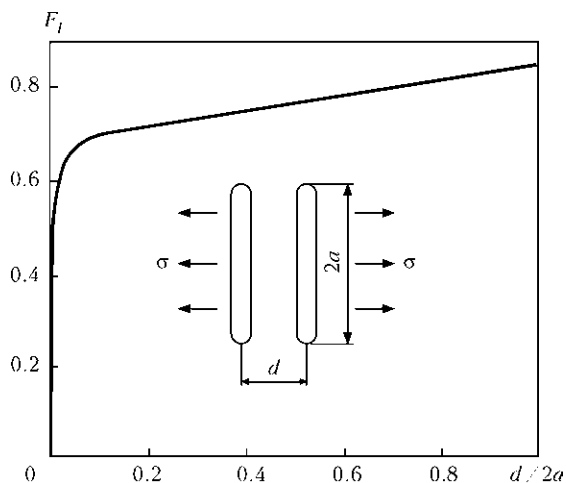


Figure 1. Dependence $F_I = K_I / (\sigma \sqrt{\pi a})$ on $d / 2a$ [4]

Table 1. Numerical results [4]

$2a/d$	F_I
0	1.0000*
0.2	0.9855*
0.4	0.9508*
0.6	0.9089*
0.8	0.8727*
1.0	0.8319
1.25	0.8037
2	0.7569
5	0.6962
10	0.6651
100	0.5846

*Plate with central crack.

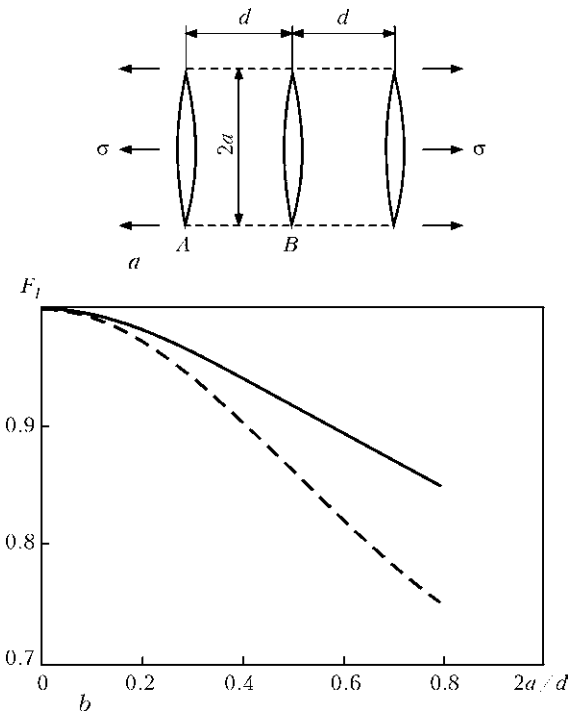


Figure 2. Uniform tension of plane with three parallel cracks of equal length along the normal to crack lines (a), and dependence of $F_{I,A}$ (solid curve) and $F_{I,B}$ (hatched) on $2a/d$ (b)

Explanation of such a fact follows from the local stress field, arising around the crack tips. Figure 3 gives the typical picture of distribution of stresses σ_{zz} in the zone of through-thickness crack $2a = 20$ mm with normal z in the strip-plate in plane $z = 0$. It is seen that on crack faces $z = 0$, $\sigma_{zz} = 0$, and then, as z rises, stresses σ_{zz} gradually increase up to 300 MPa, for those applied on the boundary $z = 500$ mm. Width of strip is $2L_x = 200$ mm, material is steel with yield point $\sigma_y = 420$ MPa. Thus, near the crack — its free faces — a field of unloading by stresses σ_{zz} forms that will, naturally, affect values K_I , if the second crack is placed into this field that is quite convincingly

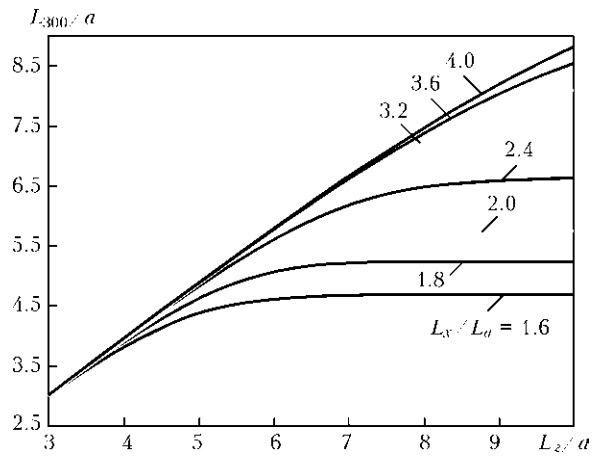


Figure 4. Extent of unloading zone along the axis $x = 0$ for isolated crack in plate of $L_z \times L_x$

demonstrated by the data in Figure 1 and Table 1. As the unloading zone has finite dimensions, at sufficiently large d the interaction between the two cracks becomes negligible.

It is characteristic that the extend of unloading zone L_σ along axis z depends on dimensions of crack $2a$ and overall dimensions of the strip $2L_z \times L_x$, that can be seen from the data in Figure 4. Such examples of interaction of parallel defects-cracks in the case of welded joints are quite numerous in practical diagnostics, for instance, a cruciform joint of elements of sufficiently large thickness t , welded by fillet welds with leg S at incomplete penetration, forming two extended (along the weld) defects of material discontinuity (cracks) of size $2a$ (Figure 5). This joint is quite well-studied both under tension (Figure 5, a) and at bending (Figure 5, b) [4], that allows these data for $K_{0,max}$ to be used both at evaluation of brittle strength, and at evaluation of growth of $2a$ value at cyclic loading [3]. In Figure 5 parameter $\varepsilon = l/t_2$, where $l = S$ is the fillet weld leg; t_2 is the thickness of uncut element — distance between parallel defects,

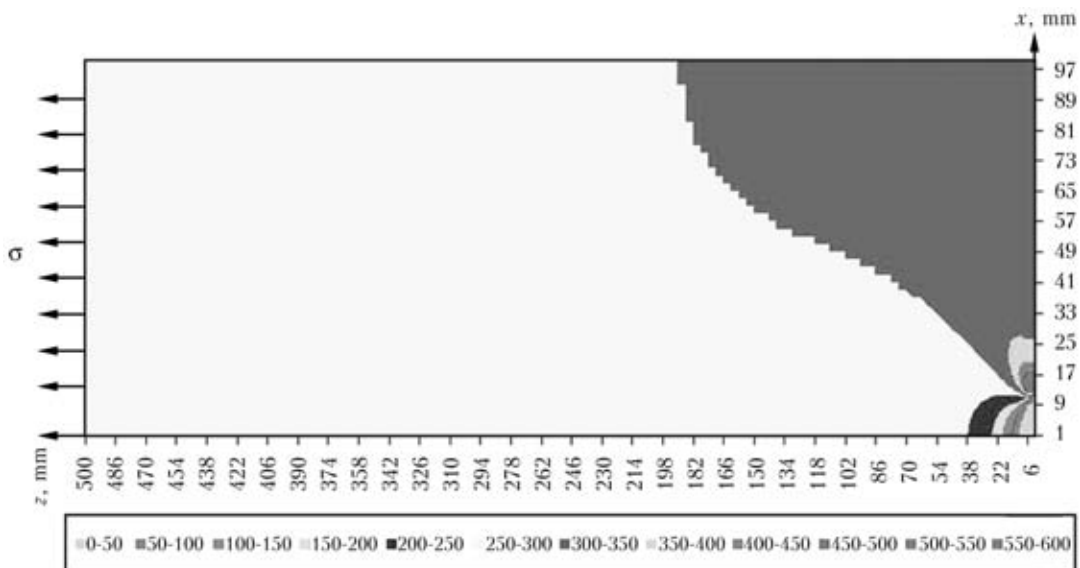


Figure 3. Unloading zone for the case of $a = 10$ mm of isolated crack in plate of $2L_z = 1000$ mm $2L_x = 200$ mm of steel with $\sigma_y = 420$ MPa and $\sigma = 300$ MPa

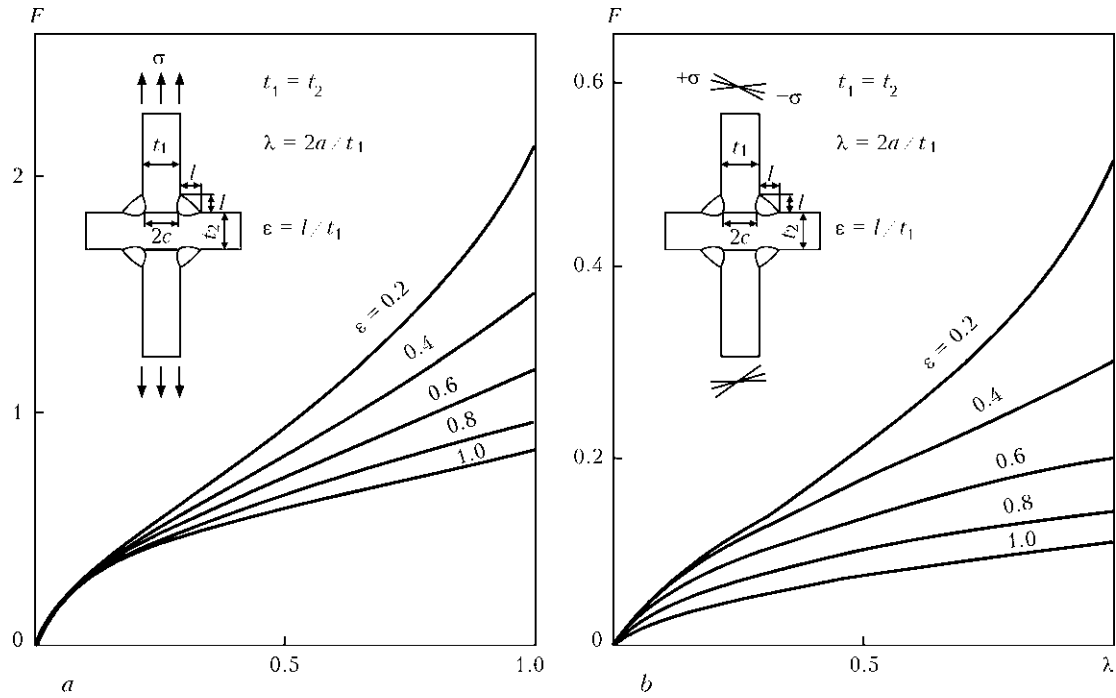


Figure 5. $F(\lambda)$ dependence ($F = K_{\theta_{max}} / \sigma \sqrt{t_1}$, $t_1 = t_2$) at tension (a) and bending (b) in cruciform joint [4]

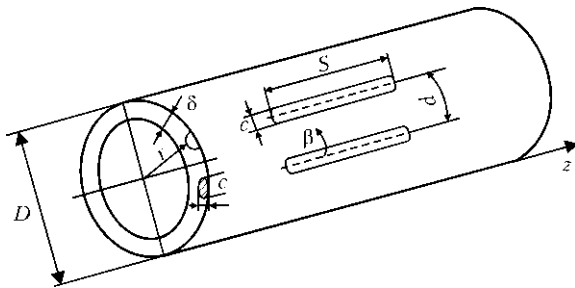


Figure 6. Schematic of cylindrical shell-pipe with longitudinal groove thinning defects

demonstrates t_2 influence on $K_{\theta_{max}}$ value at other conditions being equal, i.e. defect interaction.

Note that the effect of defect parallelism in the respective field of nominal stresses is manifested not only for crack-like defects, but also for thinning defects. For instance, in cylindrical shell-pipe two groove thinning defects along the pipe generatrix, at their parallel location (Figure 6), interacting with each other, in the case of in-pipe pressure P , lower the critical pressure in the pipe, depending on distance between defects d . Results of numerical calculations using the procedure from work [5] are given below. Defects with overall dimensions $s \times c \times a$ (a is the

maximum defect depth) are modeled by a semi-ellipsoid on pipe surface, i.e. defect surface is described in the coordinate system r, β, z by the equation

$$\left(\frac{2z}{s}\right)^2 + \left(\frac{2\beta r}{c}\right)^2 + \left(\frac{R-r}{a}\right)^2 = 1 \quad (2R = D). \quad (1)$$

At internal pressure maximum circumferential stresses $\sigma_{\beta\beta}$ arise in midplanes $\beta = 0$ and $\beta = d/R$. Fracture probability in these planes of area F according to [5] is determined by Weibull dependence

$$p = 1 - \exp \left[- \int_F \left(\frac{\sigma_{\beta\beta}(0, r, z) - A}{B} \right)^4 dF \right] \quad (2)$$

at $\sigma_{\beta\beta}(0, r, z) > A$,

where A, B are the Weibull distribution parameters experimentally determined for this material. If experimental data from [2] are used, then $A = (\sigma_y + \sigma_t) / 2$ can be assumed for a steel pipe, for isolated defect in a pipe with $D = 1420$ mm, $\delta = 28$ mm, $A = 500$ MPa, $\sigma_y = 440$ MPa, respectively.

Respective calculation of the stress-strain state for the above initial data shows that at $P = 9$ MPa in the

Table 2. Results of calculation of failure probability p by (2) for groove thinning defects (see Figure 6) at different distances between defects d and pressures P

Variant #	Pressure P , MPa	One defect	Two defects		
			$d = 90$ mm	$d = 60$ mm	$d = 48$ mm
1	7	0.00075	0	0	0
2	8	0.0068	0.0013	0.0010	0.0010
3	9	0.05	0.0072	0.0057	0.0049
4	10	0.16	0.0290	0.0268	0.0200



case of an isolated defect at $s = 66$ mm, $c = 40$ mm, $a = 14$ mm, $p \approx 0.05$ according to [2] that corresponds to $B = 470$ MPa. Considering such B value, p values were calculated by (2), which are given in Table 2 at different d and P .

CONCLUSIONS

1. Interaction of defects at force loading of welded structures largely depends on defect geometry and their position relative to the direction of force load application.

2. The most studied is the interaction of material discontinuity defects of the type of cracks and thinning, which are located in one loaded section of the item, so-called collinear defects. There are the respective schematics of combining such defects, depending on overall dimensions of defects and distance between them.

3. Unlike collinear defects, parallel defects of the type of cracks and groove thinning, located in differ-

ent, but parallel sections of the item, usually unload each other. Therefore, they are less critical when they draw closer to each other, compared to similar collinear defects.

4. At present, owing to development of information technologies and computer engineering means, it is possible to assess the interaction of the found defects in welded structures based on the respective solutions of deformation mechanics for elasto-plastic continua with cracks or thinning defects.

1. *MR-125-01-90*: Calculation of stress intensity factors and section weakening for defects in welded joints. Kiev.
2. (2000) *Fitness-for-service*: American Petroleum Institute Recommended Practice 579.
3. Makhnenko, V.I. (2006) *Safe operation resource of welded joints and assemblies of current structures*. Kiev: Naukova Dumka.
4. (1999) *Reference book on stress intensity factors*. Vol. 1 and 2. Ed. by Yu. Murakavi. Moscow: Mir.
5. Makhnenko, V.I., Velikoivanenko, E.A., Rozyinka, G.F. et al. (2010) Improvement of method for estimation of the risk of fracture within the thinning zone on walls of main pipelines. *The Paton Welding J.*, 5, 10–14.

APPLICATION OF POWDERS OF COBALT AND NICKEL ALLOYS FOR PLASMA SURFACING OF EXHAUST VALVES OF INTERNAL COMBUSTION ENGINES

E.F. PEREPLYOTCHIKOV

E.O. Paton Electric Welding Institute, NASU, Kiev, Ukraine

Properties of alloys based on cobalt and nickel for plasma surfacing of exhaust valves of gasoline and diesel engines of cars and lorries as well as engines of diesel locomotives and ships are considered. Recommendations on application of powders of various compositions for valve surfacing are given.

Keywords: *plasma-powder surfacing, powders of cobalt alloys, powders of nickel alloys, valves of internal combustion engines*

Exhaust valves of internal combustion engines (ICE) suffer from high temperature cycling, power loads as well as corrosion in operation. Operating temperature of valve head of ICE of a car reaches 700 °C and that for a lorry makes 800 °C. Multiple heating and cooling, non-uniform distribution of temperature over a valve section and cyclic power loading result in damage of contact surface of a valve face. Surfacing of the face by alloys with high heat resistance, thermal stability, hot hardness and corrosion resistance is the most effective method for a burn-out and wear-out preventing.

Nickel and cobalt based alloys are used for surfacing of contact surfaces of the faces depending on operating conditions of ICE valves. Cobalt-chromium-tungsten alloys (stellites) Nos. 6 and 12 as well as stellite F and VZK (domestic analog of stellite No.6)

(Table 1) are the most widely used for surfacing of the valves among the stellites.

All these alloys differ by high wear resistance, thermal stability and heat resistance at standard and elevated temperatures as well as high corrosion resistance in many aggressive media. Corrosion resistance of the stellites exceeds approximately 10 times resistance of steel used for ICE valves. It is usually evaluated on weight loss in molten plumbic oxide PbO at 910 °C in engine construction.

Characteristic of the stellites is the possibility to preserve sufficient hardness at high temperatures. As can be seen from Figure 1, hardness of alloy of stellite F has the most intensive decrease starting from 500 °C. Properties of solid solution and carbide eutectics as well as relationship of these main constituents determine hardness being an integral characteristic of the stellites. Significant decrease of hardness of F stellite alloy at 700 °C is related with softening of the solid solution enriched with nickel.